

A wall-less poly(vinyl alcohol) cryogel flow phantom with accurate scattering properties for transcranial Doppler ultrasound propagation channels analysis

Alexander J. Weir¹, Robin Sayer², Cheng-Xiang Wang³ and Stuart Parks⁴

Abstract—Medical phantoms are frequently required to verify image and signal processing systems, and are often used to support algorithm development for a wide range of imaging and blood flow assessments. A phantom with accurate scattering properties is a crucial requirement when assessing the effects of multi-path propagation channels during the development of complex signal processing techniques for Transcranial Doppler (TCD) ultrasound. The simulation of physiological blood flow in a phantom with tissue and blood equivalence can be achieved using a variety of techniques. In this paper, poly (vinyl alcohol) cryogel (PVA-C) tissue mimicking material (TMM) is evaluated in conjunction with a number of potential scattering agents. The acoustic properties of the TMMs are assessed and an acoustic velocity of 1524ms^{-1} , an attenuation coefficient of $(0.49) \times 10^{-4}\text{dBm}^{-1}\text{Hz}^{-1}$, a characteristic impedance of $(1.72) \times 10^6\text{Kgm}^{-2}\text{s}^{-1}$ and a backscatter coefficient of $(1.12) \times 10^{-28}\text{f}^4\text{m}^{-1}\text{Hz}^{-4}\text{sr}^{-1}$ were achieved using 4 freeze-thaw cycles and an aluminium oxide (Al_2O_3) scattering agent. This TMM was used to make an anatomically realistic wall-less flow phantom for studying the effects of multipath propagation in TCD ultrasound.

I. INTRODUCTION

TCD ultrasound [1] [2] is a low frequency (2 MHz) pulsed Doppler ultrasound system used to interrogate the intra-cranial arterial system for detection of micro embolic signals (MES) for the diagnosis and prediction of embolic complications in stroke-risk patients. In recent years there has been much interest in the use of chirp signals, coded excitation and pseudo noise (PN) codes [3]–[6] which use coded pulse sequences and digital signal processing (DSP) techniques to improve the sensitivity and reliability of detection, and subsequently the ability to track blood flow and emboli motion in TCD systems. However, lessons from radio communications [7] have shown that successful design of such techniques rely upon a thorough knowledge of the radio channel and the multipath propagation effects resulting from the reflection, diffraction and scattering of the radio

frequency (RF) signal by the medium. A flow phantom with tissue and blood equivalence is, therefore, an important tool when evaluating simulation models and signal processing techniques for TCD ultrasound.

There are a number of commercially available flow phantoms. These are commonly based on TMMs such as low density reticulated foam, gelatin and agar; the acoustic and mechanical properties of which are mostly well known over 2-10 MHz [8]. However PVA-C offers a number of advantages over traditional TMMs; it's non-toxic, maintains long-term structural and acoustic stability and can form vascular models without the use of additional tubing, such as silicon rubber, latex etc. This last point is important, since unwanted artefacts in the received signal can be introduced by the poor acoustic properties of tubing materials. For these reasons, PVA-C TMMs have emerged from initial use in magnetic resonance imaging (MRI) and are now widely employed in brain, vessel and breast ultrasound phantoms [9].

In this study, the suitability of a PVA-C TMM is assessed for production of a TCD blood flow phantom for analysis and verification of scattering channel models [10]. In order to improve the attenuation and backscattering properties of PVA-C, a number of common scattering agents were tested; namely silicon carbideⁱ, graphiteⁱⁱ and aluminium oxideⁱⁱⁱ particles. The acoustic velocity, attenuation, characteristic impedance and backscatter coefficient of the TMMs were assessed. The results of this evaluation are reported and a wall-less PVA-C flow phantom design is described.

This paper is organised as follows: Section II describes the materials and methods used to analyse the acoustic properties of the TMM. Section III describes the acoustic test results of the TMM materials. Section IV describes the design of a TCD flow phantom using the 4-cycle aluminium oxide TMM. The paper concludes in section V and provides acknowledgements in section VI.

II. MATERIALS AND METHODS

An experiment was designed to test the acoustic properties of each candidate TMM sample at a centre frequency of 2.08 MHz against the standards

ⁱSilicon carbide powder (Grit 400, 20μ particle size), supplied by Logitech Ltd, Erskine Ferry Road, Old Kilpatrick, Glasgow G60 5EU.

ⁱⁱGraphite powder (Mesh size 340<, 44μ particle size), supplied by Easy Composites Ltd, Unit 39, Park Hall Business Village, Longton, Stoke on Trent, Staffordshire ST3 5XA.

ⁱⁱⁱAluminium oxide powder (3μ particle size), supplied by Logitech Ltd, Erskine Ferry Road, Old Kilpatrick, Glasgow G60 5EU.

¹A.J. Weir is with the Medical Devices Unit, Department of Clinical Physics, Southern General Hospital, Glasgow, United Kingdom and the School of Engineering and Physical Science, Heriot-Watt University, Edinburgh, United Kingdom. alexander.weir@nhs.net

²R. Sayer is with the Medical Devices Unit, Department of Clinical Physics, Western Infirmary, Glasgow, United Kingdom. robin.sayer@nhs.net

³C.-X. Wang is with School of Engineering and Physical Science, Heriot-Watt University, Edinburgh, United Kingdom. cheng-xiang.wang@hw.ac.uk

⁴S. Parks is with the Medical Devices Unit, Department of Clinical Physics, Southern General Hospital, Glasgow, United Kingdom. stuart.parks@nhs.net

recommended by IEC 61685 [11]: TMMs should have an acoustic velocity of $1540(\pm(15))ms^{-1}$, an attenuation coefficient of $(0.5 \pm 0.05) \times 10^{-4} f dBm^{-1} Hz^{-1}$, a characteristic acoustic impedance of $(1.6 \pm 0.16) \times 10^6 K gm^{-2} s^{-1}$ and a backscatter coefficient of $(1 - 4) \times 10^{-28} f^4 m^{-1} Hz^{-4} sr^{-1}$.

A. Preparation of Tissue-Mimicking Materials (TMMs)

PVA is a water-soluble synthetic polymer. An aqueous solution of PVA was prepared by mixing 10% by weight of PVA powder^{iv} with sterile distilled water at room temperature. To this solution, 0.01% benzalkonium chloride^v was added to prevent microbial invasion in the phantom. The solution was gently heated and mixed until it became a thick, clear liquid (fig. 1). When heating the solution, care must be taken to prevent the temperature rising above 98 °C in order to prevent aeration due to boiling. The solution is then allowed to cool to room temperature. Once cooled, the solution is mixed with the desired scattering agent (1% by weight of the aluminium, graphite and silicon carbide powders) and then degassed in a vacuum chamber.

The final stage of PVA-C TMM preparation is freeze-thawing the solution to create a solid phantom. This was performed in a programmable thermo-cycler^{vi} that was configured to automatically perform 4, 6 and 8 cycles of 12 hours freezing to -20 °C and 12 hours thawing to +20 °C. In total, 12 candidate TMMs were prepared; for each of the (4, 6 and 8) cycles, test samples were produced for control (no scattering agent), aluminium, graphite and silicon carbide. Examples of the TMM test samples are shown in (fig. 2).



Fig. 1: An aqueous solution of 10% by weight PVA in water.



Fig. 2: PVA-C TMM after 4 freeze-thaw cycles samples for control, silicon carbide (SiC), graphite and aluminium oxide (AlO).

B. Measurements of acoustic velocity, attenuation coefficient, characteristic acoustic impedance and backscatter coefficient

The measurement methods followed were based on the techniques described by *Browne et al* [12]. The acoustic velocity, attenuation coefficient and backscatter coefficient were measured using the ultrasonic test system shown in fig. 3. The test system consisted of an Olympus NDT immersion transducer (A306S-SU) with a centre frequency of 2.08 MHz mounted upon a XYZ motion stage, an immersion water tank filled with de-gassed water, a programmable pulser-receiver (Utex UT340), a digital storage oscilloscope (Tektronix TPS2024B) and a personal computer (PC) with supporting software developed for Matlab^{vii} for control of the motion stage and analysis of the pulse-echo observations.

The pulse-echo technique uses a single transducer operat-

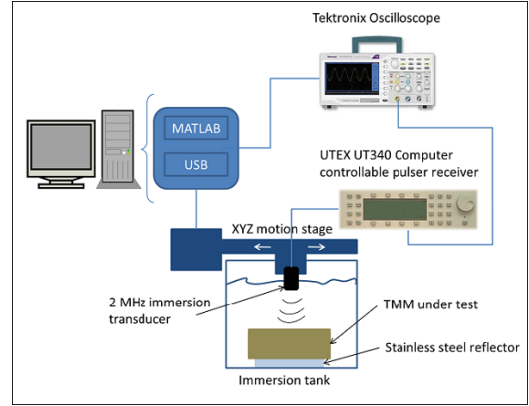


Fig. 3: Ultrasonic pulse-echo test system.

ing sequentially in transmit and receive modes. The pulser-receiver was configured to drive the transducer at 100 V with a pulse repetition frequency of 200 Hz. The induced pulse was reflected from a highly polished stainless steel reflector in the base of the immersion tank. The motion stage was programmed to position the transducer over an area of 8 mm by 8 mm at intervals of 1 mm, allowing measurements to be spatially averaged. At each position of the transducer, the reflected RF signal was sampled at 25 MHz using the digital storage oscilloscope and post-processed on a PC using Matlab scripts developed in-house for this purpose. All measurements were conducted with a water temperature of $20^\circ C \pm 1^\circ C$.

1) *Calculating the acoustic velocity:* The acoustic velocity in the TMM sample was determined by measuring the time difference between the RF pulse and its echo from the stainless steel reflector with and without the TMM sample in place. This was calculated using the equation,

$$c_s = \frac{c_w}{1 + \Delta t \frac{c_w}{d}}, \quad (1)$$

where c_s was the acoustic velocity in the sample, c_w was the reference speed of sound in degassed water with no sample in place, d was the depth of the TMM sample (measured using digital callipers) and Δt was the time shift of the RF pulse and echo with the sample in place. The reference speed of sound, c_w , was calculated using the equation

$$c_w = \frac{2d}{\Delta t}. \quad (2)$$

The calculated value of c_w was found to be within 0.25% of the expected value at $T^\circ C$ using the formula for the speed of sound in pure water as a function of temperature derived by *Bilaniuk et al* [13].

^{iv}Poly (vinyl alcohol) 99+% hydrolysed, product 341584, Sigma-Aldrich UK company Ltd. Dorset, England.

^vBenzalkonium chloride solution, product 63249, Sigma-Aldrich UK company Ltd. Dorset, England.

^{vi}Automated thermo-cycler, developed by the Department of Clinical Physics & Bioengineering, NHS Greater Glasgow and Clyde.

^{vii}MathWorks Inc., Natick, MA, United States of America.

2) *Calculating the acoustic attenuation coefficient:* The acoustic attenuation coefficient (α) of the sample was calculated as the log difference of the magnitudes of the gated RF echo using the equation

$$\alpha = \frac{-20}{d} \log_{10} \frac{|V_s|}{|V_w|}, \quad (3)$$

where $|V_s|$ was the magnitude of the gated RF echo with the sample in place and $|V_w|$ was the magnitude of the gated RF echo through degassed water. The magnitudes were calculated using a 256-point discrete Fourier transform.

3) *Calculating the acoustic backscatter coefficient:* The acoustic backscatter coefficient (η) of the sample was calculated as the difference of the power spectra of the gated RF echo using the formulation derived by *Chen et al* [14] for flat transducers, by the equation

$$\eta \cong \begin{cases} \frac{\langle |V_s|^2 \rangle}{|V_w|^2} \cdot \frac{ka^2}{1.4\pi \exp\left[\left(\frac{\bar{r}}{r_0}\right)^{\frac{1}{2}}\right]}, & \frac{\bar{r}}{r_0} < 1, \\ \frac{\langle |V_s|^2 \rangle}{|V_w|^2} \cdot \frac{ka^2}{1.4\pi \cdot 4E_\infty}, & \frac{\bar{r}}{r_0} > 1, \end{cases} \quad (4)$$

where $\langle |V_s|^2 \rangle$ was the mean power of the gated RF echo with the sample in place, $|V_w|^2$ was the power of the gated RF echo through degassed water, k is the wave number, a is the radius of the transducers active element, \bar{r} is the mean distance from the transducer surface to the sample volume, r_0 is the Rayleigh distance of the transducer, and l is the length of the windowed backscatter signal.

4) *Calculating the acoustic impedance:* The acoustic impedance (z) was calculated using the formula $z = \rho \times c_s$, where ρ was the measured density of the sample and c_s was acoustic velocity calculated for the sample.

III. RESULTS

A summary of the acoustic properties of the TMM samples are shown in Table I and the effects of varying the number of freeze-thaw cycles on the acoustic velocity, attenuation coefficient and the backscatter coefficient are shown in fig. 4, fig. 5 and fig. 6 respectively.

The acoustic velocities for the 4-cycle control samples shown on fig. 4 are generally slightly lower than previously reported [9] and this seems the case for all the velocity measures. However the general trend is consistent, showing that increasing the number of freeze-thaw cycles results in an increase in acoustic velocity through the sample. The acoustic velocity measured in the 8-cycle graphite sample seems outside the general trend, nevertheless the acoustic velocities measured are mostly within IEC limits; $1540(\pm(15))ms^{-1}$. The 4 and 6-cycle aluminium oxide samples fall just outside the lower limit. However, at $1524ms^{-1}$, the 4-cycle sample is thought to be within acceptable measurement tolerances given that all velocities were slightly lower than anticipated.

The attenuation coefficient results shown in fig. 5 fall broadly within the anticipated range for the number of freeze-thaw cycles at an insonation frequency of 2 MHz [8] [9]. The introduction of scattering agents can be seen to increase the attenuation coefficient of PVA-C, and this effect can

similarly be observed by increasing the number of freeze-thaw cycles in the control samples. The results for silicon carbide fall outside of the general trend suggesting there may be a problem with this sample, and the attenuation coefficients measured for all samples, except that of 4-cycle aluminium oxide, fall outside the recommended IEC standard of $(0.5 \pm 0.05) \times 10^{-4} f dBm^{-1} Hz^{-1}$. This highlights the main problem with PVA-C based phantoms; it is difficult to obtain the recommended attenuation coefficient, but shows that it may be possible to balance the acoustic velocity and attenuation coefficient requirements using a scattering agent such as aluminium oxide.

Finally, the backscatter coefficient results in fig. 6 show that introducing scattering agents can be seen to reduce the backscatter coefficient of PVA-C, and this effect increases with the number of freeze-thaw cycles in the control samples. Once again, the results for silicon carbide fall outside of the general trend, while the aluminium oxide sample continues to show promise. The trend observed in these results shows that increasing the number of freeze-thaw cycles beyond 6 will result in a backscatter coefficient below the requirement of $(1 - 4) \times 10^{-28} f^4 m^{-1} Hz^{-4} sr^{-1}$. Notably, the IEC standard places less emphasis on the backscatter coefficient requirement, particularly at frequencies below 4 MHz.

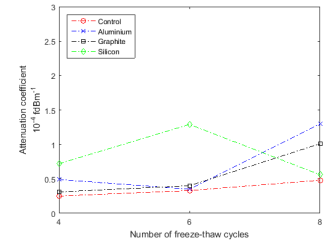
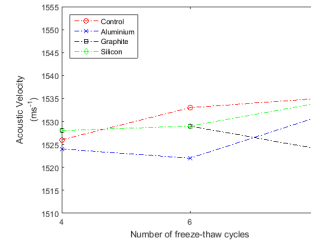


Fig. 4: Acoustic velocity for 4,6 and 8-cycle test samples.

Fig. 5: Attenuation coefficient for 4,6 and 8-cycle test samples.

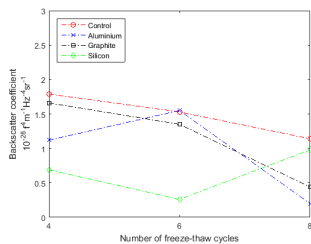


Fig. 6: Backscatter coefficient for 4,6 and 8-cycle test samples.

Fig. 7: The TCD Doppler flow phantom perspex mould.

IV. PREPARATION OF A TRANSCRANIAL DOPPLER (TCD) FLOW PHANTOM

For durability, structural stability and acoustic properties, PVA-C provides a highly suitable TMM from which to construct an anatomically realistic wall-less flow phantom. An example of a system for investigation of the effects of multipath propagation in TCD ultrasound systems is shown in fig. 8. As mentioned previously, a significant advantage of PVA-C over alternative TMMs, such as Agar and Gelatin, is its ability to form a wall-less channel during the freeze-thaw

TABLE I: Measured tissue mimicking material parameters

Scattering Agent	No. freeze-thaw cycles	Acoustic Velocity (v) $m \cdot s^{-1}$	Attenuation coeff. (α) $(\times 10^{-4}) f dB m^{-1} Hz^{-1}$	Acoustic Impedance (Z) $(\times 10^6) Kg m^{-2} s^{-1}$	Backscatter coeff. (η) $(\times 10^{-28}) f^4 m^{-1} Hz^{-4} sr^{-1}$
IEC 61685 TMM parameters [11]	—	1540 ± 15	(0.5 ± 0.05)	(1.6 ± 0.16)	1
Control (none)	4 cycles	1526	0.25	1.72	1.79
	6 cycles	1533	0.33	1.75	1.53
	8 cycles	1535	0.48	1.79	1.14
Silicon Carbide	4 cycles	1528	0.72	1.71	0.69
	6 cycles	1529	1.29	1.73	0.26
	8 cycles	1534	0.56	1.75	0.98
Graphite	4 cycles	1528	0.31	1.70	1.66
	6 cycles	1529	0.40	1.74	1.35
	8 cycles	1524	1.05	1.77	0.44
Aluminium Oxide	4 cycles	1524	0.49	1.72	1.12
	6 cycles	1522	0.35	1.73	1.55
	8 cycles	1529	1.30	1.76	0.20

[†] The Attenuation coeff. and Backscatter coeff. measurement units are expressed in relation to insonation frequency for comparison with the IEC 61685 TMM parameter recommendations. However all experimental works reported here were performed at 2.08 MHz and the actual nature of the frequency dependence of this technique was not determined.

process, avoiding the requirement for vessel wall tubing. The perspex mould, shown in fig. 7, provides an example of vessel geometry and dimensions conforming to IEC standards. To reduce the effects of noise caused by signal reflections from the phantom walls, the mould can be lined with low profile, coarse synthetic grass^{viii} to provide acoustic damping and improve the signal-to-noise ratio (SNR).

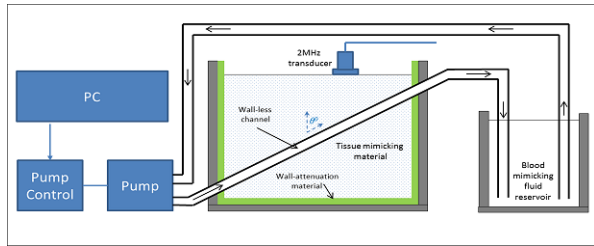


Fig. 8: A TCD ultrasound flow phantom system.

V. CONCLUSION

In this paper PVA-C was evaluated with a number of potential scattering agents for use as a TMM in a Doppler flow phantom. Although the material benefits of PVA-C are clear, it requires additional scattering agents to achieve acoustic properties consistent with recommended standards. Tests using common scattering agents showed that a 4-cycle TMM with 1% aluminium oxide can achieve acoustic properties that are agreeable with IEC standards, and can be used in wall-less flow phantoms. Subsequent preparations have shown this process to be repeatable in small volumes, however the overall velocity, attenuation and backscatter results suggest it may be difficult to achieve truly consistent results with PVA-C with different laboratory production equipment and its possible that some minor differences in production account for the slightly lower acoustic velocities observed in this paper. Furthermore, the inconsistent results observed with silicon carbide are thought to be caused by difficulty in achieving an even dispersal of powder in aqueous solution, resulting in an inhomogeneous TMM. To guarantee consistent results, it is recommended that careful adherence is given to each step in preparation of the TMM.

^{viii}Synthetic grass (6 mm/flat blade), Express Grass, Trinity Trading Estate, Sittingbourne, Kent ME10 2PG

VI. ACKNOWLEDGEMENTS

I would like to thank Dr Amanda Watson at the Dept. Clinical Physics, NHS Greater Glasgow and Clyde for guidance during the preparation of phantom gels. I would also like to thank Prof Tony Gachagan and Mr Walter Galbraith at the University of Strathclyde for providing the pulse-echo test system for the experimental work.

REFERENCES

- [1] R. Aaslid, T.-M. Markwalder, and H. Nornes, "Noninvasive transcranial doppler ultrasound recording of flow velocity in basal cerebral arteries," *Journal of neurosurgery*, vol. 57, no. 6, pp. 769–774, 1982.
- [2] H. S. Markus, "Transcranial doppler ultrasound," *Journal of Neurology, Neurosurgery & Psychiatry*, vol. 67, no. 2, pp. 135–137, 1999.
- [3] J. Cowe, J. Gittins, and D. H. Evans, "Improving performance of pulse compression in a doppler ultrasound system using amplitude modulated chirps and wiener filtering," *Ultrasound in medicine & biology*, vol. 34, no. 2, pp. 326–333, 2008.
- [4] J. Cowe, E. Boni, S. Ricci, P. Tortoli, and D. Evans, "Coded excitation can provide simultaneous improvements in sensitivity and axial resolution in doppler ultrasound systems," in *Ultrasonics Symposium (IUS), 2010 IEEE*, pp. 2286–2290, IEEE, 2010.
- [5] X. Lei, Z. Heng, and G. Shangkai, "Barker code in tcd ultrasound systems to improve the sensitivity of emboli detection," *Ultrasound in medicine & biology*, vol. 35, no. 1, pp. 94–101, 2009.
- [6] J. Li, X. Diao, K. Zhan, and Z. Qin, "A full digital design of tcd ultrasound system using normal pulse and coded excitation," in *1st Global Conference on Biomedical Engineering & 9th Asian-Pacific Conference on Medical and Biological Engineering*, pp. 136–139, Springer, 2015.
- [7] M. Patzold, *Mobile fading channels*. John Wiley & Sons, Inc., 2003.
- [8] P. R. Hoskins, "Simulation and validation of arterial ultrasound imaging and blood flow," *Ultrasound in medicine & biology*, vol. 34, no. 5, pp. 693–717, 2008.
- [9] K. Surry, H. Austin, A. Fenster, and T. Peters, "Poly (vinyl alcohol) cryogel phantoms for use in ultrasound and mr imaging," *Physics in medicine and biology*, vol. 49, no. 24, p. 5529, 2004.
- [10] A. Weir, C.-X. Wang, and S. Parks, "3-d half-spheroid models for transcranial doppler ultrasound propagation channels," in *Biomedical and Health Informatics (BHI), 2014 IEEE-EMBS International Conference on*, pp. 728–731, IEEE, 2014.
- [11] I. E. Commission *et al.*, *Ultrasonics: Flow Measurement Systems; Flow Test Object; International Standard*. IEC, 2001.
- [12] J. Browne, K. Ramnarine, A. Watson, and P. Hoskins, "Assessment of the acoustic properties of common tissue-mimicking test phantoms," *Ultrasound in medicine & biology*, vol. 29, no. 7, pp. 1053–1060, 2003.
- [13] N. Bilaniuk and G. S. Wong, "Speed of sound in pure water as a function of temperature," *The Journal of the Acoustical Society of America*, vol. 93, no. 3, pp. 1609–1612, 1993.
- [14] X. Chen, D. Phillips, K. Q. Schwarz, J. G. Mottley, and K. J. Parker, "The measurement of backscatter coefficient from a broadband pulse-echo system: a new formulation," *Ultrasonics, Ferroelectrics, and Frequency Control, IEEE Transactions on*, vol. 44, no. 2, pp. 515–525, 1997.